



HAL
open science

**Amphiphilic and segmented polyurethanes based on
poly(ϵ -caprolactone)diol and
poly(2-ethyl-2-oxazoline)diol: Synthesis, properties, and
a preliminary performance study of the 3D printing**

Leonardo Bueno Bronzeri, Cony Gauche, Leslie Gudimard, Edwin-Joffrey
Courtial, Christophe Marquette, Maria Isabel Felisberti

► **To cite this version:**

Leonardo Bueno Bronzeri, Cony Gauche, Leslie Gudimard, Edwin-Joffrey Courtial, Christophe Marquette, et al.. Amphiphilic and segmented polyurethanes based on poly(ϵ -caprolactone)diol and poly(2-ethyl-2-oxazoline)diol: Synthesis, properties, and a preliminary performance study of the 3D printing. *European Polymer Journal*, 2021, 151, pp.110449. 10.1016/j.eurpolymj.2021.110449 . hal-03364503

HAL Id: hal-03364503

<https://hal.science/hal-03364503>

Submitted on 4 Oct 2021

HAL is a multi-disciplinary open access archive for the deposit and dissemination of scientific research documents, whether they are published or not. The documents may come from teaching and research institutions in France or abroad, or from public or private research centers.

L'archive ouverte pluridisciplinaire **HAL**, est destinée au dépôt et à la diffusion de documents scientifiques de niveau recherche, publiés ou non, émanant des établissements d'enseignement et de recherche français ou étrangers, des laboratoires publics ou privés.

Amphiphilic and segmented polyurethanes based on poly(ϵ -caprolactone)diol and poly(2-ethyl-2-oxazoline)diol: Synthesis, properties, and a preliminary performance study of the 3D printing
Marquette Christophe, Maria Felisberti, Leonardo Bueno Bronzeri, Cony Gauche, Leslie Gudimard, Edwin-Joffrey Courtial, Christophe Marquette, Gustavo Abraham, Mattia Sponchioni, Suzana Cakić, et al.

► **To cite this version:**

Marquette Christophe, Maria Felisberti, Leonardo Bueno Bronzeri, Cony Gauche, Leslie Gudimard, et al.. Amphiphilic and segmented polyurethanes based on poly(ϵ -caprolactone)diol and poly(2-ethyl-2-oxazoline)diol: Synthesis, properties, and a preliminary performance study of the 3D printing. European Polymer Journal, Elsevier, 2021, 151, pp.110449. 10.1016/j.eurpolymj.2021.110449 . hal-03364503

HAL Id: hal-03364503

<https://hal.archives-ouvertes.fr/hal-03364503>

Submitted on 4 Oct 2021

HAL is a multi-disciplinary open access archive for the deposit and dissemination of scientific research documents, whether they are published or not. The documents may come from teaching and research institutions in France or abroad, or from public or private research centers.

L'archive ouverte pluridisciplinaire **HAL**, est destinée au dépôt et à la diffusion de documents scientifiques de niveau recherche, publiés ou non, émanant des établissements d'enseignement et de recherche français ou étrangers, des laboratoires publics ou privés.

Materials Science & Engineering C

Amphiphilic and segmented polyurethanes based on poly(ϵ -caprolactone) and poly(2-ethyl-2-oxazoline): Synthesis, properties, and 3D printing --Manuscript Draft--

Manuscript Number:	
Article Type:	Research Paper
Keywords:	AMPHIPHILIC, POLYURETHANE, SYNTHESIS, PROPERTIES, 3D PRINTING, Biocompatibility
Corresponding Author:	Maria Isabel Felisberti, PhD University of Campinas Campinas, SP BRAZIL
First Author:	Leonardo Bueno Bronzeri, BSc
Order of Authors:	Leonardo Bueno Bronzeri, BSc Cony Gauche, PhD LESLIE GUDIMARD EDWIN-JOFFREY COURTIAL, PhD CHRISTOPHE MARQUETTE, PhD Maria Isabel Felisberti, PhD
Abstract:	<p>Polyurethanes (PU) have a wide variety of applications due to possessing tailored properties which can be imparted by composition. The combination of polyols in different ratios provide specific properties for the segmented PU, such as mechanical strength, elasticity, hydrophilicity and so on. In this work, amphiphilic and segmented polyurethanes, based on poly(ϵ-caprolactone) (PCL) and poly(2-ethyl-2-oxazoline) (PEtOx) as polyols at variable mass fractions, were synthesized by a two-step route and characterized according to composition, molar mass, thermal, dynamic mechanical, and rheological properties. Polyurethanes with molar masses ranging from 17.9 to 39.6 kDa, and a molar mass dispersity in the range of 2.0 – 4.0, are capable of swelling in water, with the swelling coefficient being modulated by the polyurethane composition and by the temperature because of the lower critical solubility temperature (LCST) behavior of PEtOx in an aqueous medium. PCL and PEtOx segments are partially miscible, therefore the polyurethanes are heterogeneous, presenting a PCL/PEtOx miscible phase dispersed in a PCL rich matrix in the solid state. PU with 50% mass fraction of PEtOx presented a gelation temperature of 69°C, as determined by rheology, and was evaluated for Fused Deposition Modelling (FDM) 3D printing, showing promising features, although with a low resolution and fidelity to the computational project, mainly due to its high viscoelasticity which may be modulated by the molar mass of the polymer. Moreover, cell viability tests showed that the polyurethanes are compatible with biomedical applications.</p>
Suggested Reviewers:	<p>Gustavo Abraham, PhD Professor, Universidad Nacional de Mar del Plata Facultad de Ingenieria gabraham@fi.mdp.edu.ar Expertise: Biomedical polymers, Tissue engineering, scaffolds, segmented polyurethanes, bioresorbable polyurethanes, electrospinning.</p> <p>Mattia Sponchioni, PhD Politecnico de Milano mattia.sponchioni@polimi.it Expertise: Tissue engineering, thermo-responsive polymers, colloids, polymer reaction engineering</p> <p>Suzana M Cakić, PhD Faculty of Technology, University of Niš suzana_cakic@yahoo.com Expertise: Polymeric Materials, polymer synthesis, material characterization</p>

HIGHLIGHTS

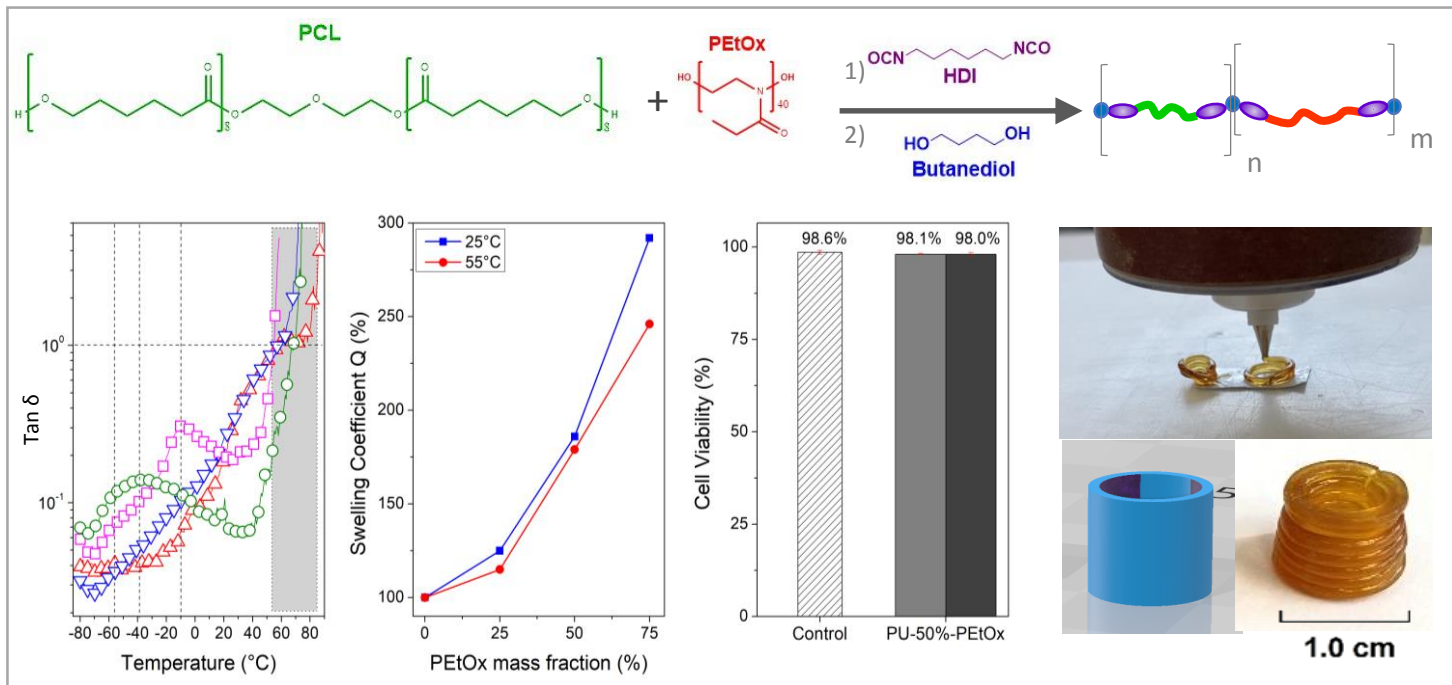
Amphiphilic polyurethanes based on PCL and PEOx were synthesized.

The polyurethanes are heterogenous in solid state due to the immiscibility of PCL and PEOx.

Polyurethanes presented a LCST behaviour similar to PEOx in aqueous medium.

Polymers are applicable for 3D printing at high temperatures.

The polyurethanes are biocompatible.



Amphiphilic and segmented polyurethanes based on poly(ϵ -caprolactone) and poly(2-ethyl-2-oxazoline): Synthesis, properties, and 3D printing

LEONARDO BUENO BRONZERI^a, CONY GAUCHE^a, LESLIE GUDIMARD^b, EDWIN-JOFFREY COURTIAL^b, CHRISTOPHE MARQUETTE^b, MARIA ISABEL FELISBERTI^a

^aInstitute of Chemistry, University of Campinas, PO Box 6154, 13084-971, Campinas –SP, Brazil

^b3d.FAB, Univ Lyon, Université Lyon 1, CNRS, INSA, CPE-Lyon, ICBMS, UMR 5246, 43, Bd du 11 novembre 1918, 69622, Villeurbanne cedex, France.

ABSTRACT

Polyurethanes (PU) have a wide variety of applications due to possessing tailored properties which can be imparted by composition. The combination of polyols in different ratios provide specific properties for the segmented PU, such as mechanical strength, elasticity, hydrophilicity and so on. In this work, amphiphilic and segmented polyurethanes, based on poly(ϵ -caprolactone) (PCL) and poly(2-ethyl-2-oxazoline) (PEtOx) as polyols at variable mass fractions, were synthesized by a two-step route and characterized according to composition, molar mass, thermal, dynamic mechanical, and rheological properties. Polyurethanes with molar masses ranging from 17.9 to 39.6 kDa, and a molar mass dispersity in the range of 2.0 – 4.0, are capable of swelling in water, with the swelling coefficient being modulated by the polyurethane composition and by the temperature because of the lower critical solubility temperature (LCST) behavior of PEtOx in an aqueous medium. PCL and PEtOx segments are partially miscible, therefore the polyurethanes are heterogeneous, presenting a PCL/PEtOx miscible phase dispersed in a PCL rich matrix in the solid state. PU with 50% mass fraction of PEtOx presented a gelation temperature of 69°C, as determined by rheology, and was evaluated for Fused Deposition Modelling (FDM) 3D printing, showing promising features, although with a low resolution and fidelity to the computational project, mainly due to its high viscoelasticity which may be modulated by the molar mass of the polymer. Moreover, cell viability tests showed that the polyurethanes are compatible with biomedical applications.

KEYWORDS: AMPHIPHILIC, POLYURETHANE, SYNTHESIS, PROPERTIES, 3D PRINTING, BIOCOMPATIBILITY

1. Introduction

Polyurethanes (PU) are very versatile polymers which present a wide range of properties and applications in different areas such as painting, coatings, insulation, automobile and aeronautical industries, biomedicine, and so on. [1–6] Particularly in the biomedical field, these materials have been widely used due to the possibility of achieving biocompatibility. [7–10] Such a characteristic is reached through the easy modulation of PU compositions, tailoring a desired polymer with specific properties for biomedical applications. In general, the chemistry of polyurethanes is simple. It consists of the combination of a polyol, a diisocyanate, and a chain extensor, which are joined together by urethane linkages. [7]

Segmented polyurethanes are random copolymers constituted, in general, by different soft and hard segments. Isocyanate fragments constitute the hard segments, providing rigidity and strength due to hydrogen bonding, while the soft segments and chain extensors impart softness and elasticity. [7,11] The soft segments are generally polyethers, polyesters, polycarbonates, or aliphatic oligoglycols. [12] The combination of several factors such as the soft and hard segment's composition, segments' length, crystallinity, polymerization techniques, etc, can be used to tune the final physical-chemical and mechanical behavior of the polymer. [13] As an example, some studies evaluated the effects of the semicrystalline/amorphous segment ratio on the mechanical performance of the PU, revealing that by increasing the semicrystalline content, the elasticity and mechanical properties were enhanced. [11,14]

The control of these properties is vital for the use of polyurethanes in tissue engineering and biomaterials. Several studies suggest that PU can be used in health improvements such as prosthesis development, tissue engineering and tissue regeneration, and controlled drug release systems. [5,15–22] Recently, elastomeric polyurethanes have been used to 3D print prostheses, implants, and systems that mimic the human system. [23–25]

Among the available polyols, poly(ϵ -caprolactone) (PCL) is a well suited polymer to be used in the preparation of segmented PU, since it is biodegradable, non-toxic and approved by the Food and Drug Administration (FDA). [8,26] It has been used for biomedical purposes in implants, drug delivery, and bone regeneration, since its time of degradation in the body is similar to that of cartilaginous tissue regeneration. [26–28] Poly(ethylene glycol) (PEG) is another polymer widely used in biomedical devices such

as hydrogels, drug delivery systems and coatings for medicaments, due to stealth properties in the body. [29] However, the human body has developed some adverse reactions to PEG, [30] and this has brought to light the use of poly(oxazoline)s (POx), in particular poly(2-methyl-2-oxazoline) and poly(2-ethyl-2-oxazoline) (PEtOx), since they present physical-chemical properties very similar to PEG. [31–33] Poly(2-alkyl-2-oxazoline)s are a class of polymers described as analogs of poly(aminoacids), named pseudo-polypeptides, [34] whose properties (e.g. cloud point in an aqueous medium [35]) can be tuned by changing the side chain of the 2-oxazoline monomer [36–39] and the initiation/termination agents. [40] They are prepared by cationic ring opening polymerization (CROP), which is a well-controlled route that allows tailoring the desired molar mass with a low polydispersity (\mathcal{D}). [38]

Segmented polyurethanes based on PCL and PEG have already been synthesized for thermo-responsive hydrogels designed for biomedical applications. Due to their amphiphilic character, PCL/PEG-based polyurethanes present great potential as carriers for acidic hydrophobic drugs, and their hydrogels have shown a temperature dependence of their water swelling capability on the polymer composition. [5,8] PEtOx, in its turn, has been combined with PCL in block copolymers and segmented PU for biomedical applications. [41–43] Bu et al. [41] synthesized a biodegradable amphiphilic polyurethane, based on PCL and PEtOx segments, capable of self-assembly to form micelles responsive to pH and reducing conditions, achieving a controlled release of doxorubicin. In the case of block copolymers, tuning the copolymer molar mass and the number of the mers of each block of a PEtOx-*b*-PCL copolymer, dictates the nature of the nanostructure morphologies, including ellipsoids, rods, or intermediate structures. [42] A brush-like PU-*graft*-PEtOx, prepared by grafting of PEtOx chains onto PCL-based PU, were synthesized by Yang et al. [43] through polycondensation, and the protein resistance was investigated. Films prepared from the brush-like PU-*graft*-PEtOx showed a lower protein adsorption than for polymers with a higher PEtOx graft density and longer PEtOx chain length.

Despite the promising combination between biocompatible PCL/PEtOx and non-toxic segments to overcome problems related to toxicity and nonspecific protein adsorption, no systematic study has been dedicated to investigating the influence of the polyols molar ratio on the properties of the segmented polyurethanes.

Nowadays, the most explored fields in 3D printing are related to biomaterials, drug release, prosthesis, and tissue engineering. [44–48] The formulation of the ink for these purposes often implies the use of living cells, although some works have reported the importance of cell-free components since the quality of the biomaterial depends on the quality of the cells and the sterility of the process. [49] The melt state is required for the layer-by-layer three-dimensional shaping on fused deposition modelling (FDM), a faster and cheaper process with reduced material loss compared with conventional injection molding techniques. [50] Therefore, thermoplastic polymers, polyurethane, and silicone elastomers are among the few options available to produce prosthesis and biomaterials. [51,52] For example, polycaprolactone 3D printed mesh has been used as an absorbable scaffold after implantation in rhinoplasty. [28] Blends of poly(ester amide) and PCL have been used for the production of 3D additive manufactured scaffolds. [53]

In this work, segmented polyurethanes, based on PCL and PEO diols and hexamethylene diisocyanate (HDI), have been synthesized via a reproducible two-step polyaddition. HDI is an aliphatic isocyanate which results in polyurethanes whose metabolites are non-toxic. [5,54,55] PEO, synthesized by cationic ring opening polymerization (CROP), and commercial PCL were used as polyols at different molar ratios to prepare PCL/PEO-based segmented polyurethanes. The polymers were structurally characterized by proton nuclear magnetic resonance (^1H NMR) and gel permeation chromatography (GPC). The thermal and mechanical properties were evaluated to study the phase behavior of the PU in the solid state, since the literature mainly reports PCL/PEO-based copolymers behavior in aqueous solutions. These polyurethanes are amphiphilic and potentially thermo-responsive due to LCST behavior of PEO. [56,57] Therefore, the water swelling capability was investigated as a function of temperature to evaluate the thermo-responsiveness of the PU. The PU was also evaluated with respect to rheology, 3D printing capability, and cell toxicity, aiming the investigation at the potential of using these materials to produce medical devices.

2. Material and Methods

2.1. Materials

2-ethyl-2-oxazoline ($\geq 99\%$, Sigma Aldrich) and acetonitrile ($> 99.9\%$, Vetec) were stirred overnight in calcium hydride and distilled before use. 1,4-dibromo-2-butene (99%, Sigma Aldrich), used as initiator for CROP, was solubilized in benzene and freeze dried. Poly(ϵ -caprolactone)-diol (2 kDa, Sigma Aldrich) was dried under vacuum at 40°C for 5 h before use. DMSO (99.9%, Synth) was passed through an alumina column and stored with a molecular sieve. Hexamethylene diisocyanate (HDI, 98%), diethyl ether (Synth, 98 %), dibutyltindilaurate (95%) and 1,4-butanediol ($>99\%$), used as a catalyst and chain extender, respectively, were purchased from Sigma Aldrich and used as received.

2.2. Synthesis of Poly(2-ethyl-2-oxazoline)

PEtOx was synthesized by cationic ring opening polymerization (CROP). 2-ethyl-2-oxazoline and 1,4-dibromo-2-butene (30 : 1 molar ratio) were introduced in a flask with dry acetonitrile (63 %, v/v) and the reaction was conducted at 80°C for 20 h, under argon atmosphere. The reaction was quenched by adding KOH methanolic solution (3 equivalent). PEtOx was purified by precipitation in cold diethyl ether and dried under vacuum. [58,59] For the polyurethane synthesis, PEtOx was further dried by azeotropic distillation from 1,2-dichloroethane solution and stored under argon atmosphere before use. [60]

2.3. Synthesis of Segmented Polyurethanes

Segmented polyurethanes based on PEtOx and PCL were synthesised by a two-step route. [8] Briefly, the desired mass ratio of dry polymers (PEtOx:PCL = 0:1, 1:3, 1:1, 3:1 and 1:0) were solubilized in DMSO (15%, m/v) containing 50 μ L of the catalyst dibutyltindilaurate. Then, HDI at an NCO:OH molar ratio of 2:1 were added under argon atmosphere. The reaction was conducted in a two-neck flask with a silicone septum, under magnetic stirring at 60°C for 24 h. The second step consisted of the addition of the chain extensor, 1,4-butanediol, followed by reaction at 60°C for 72 h. The polyurethanes were precipitated in diethyl ether, solubilized in ethanol/acetone 1:1 (v/v) and finally, precipitated in cold diethyl ether. Films were obtained by solvent

casting from the polymer solution (38%, m/v) in ethanol/acetone 1:1 (v/v) and dried under N₂ flow.

2.4. Characterization

¹H NMR spectra of the polyurethanes and precursors (PEtOx and PCL) were acquired using a Bruker Advanced III NMR 500 MHz spectrometer (Germany) instrument. Analysis conditions were: 25°C and 11.7 Tesla, pulse interval 3.0 s, 16 scans, 0.3 Hz FID resolution, and 9.0 mg samples dissolved in 0.55 mL of CDCl₃. The hydroxyl indices of PEtOx (0.504 mmol OH/g) and PCL (0.978 mmol OH/g) were calculated from the ¹H NMR spectra, according to the methodology described elsewhere. [61]

Gel permeation chromatography (GPC) analyses were conducted using a Viscotek GPC max VE 2001 equipment (Worcestershire, UK) equipped with a refraction index (RI) detector (Viscotek VE 3580) and three columns (Shodex KD-806 M) with 80 mm x 30 cm dimensions, operating at 60°C, using a DMF/LiCl solution as the eluent at a flow rate of 1 mL min⁻¹, and polystyrene standards (Malvern) for calibration. All samples were prepared at 5 mg mL⁻¹ in DMF/LiCl (10 mmol L⁻¹).

Thermogravimetric analyses (TGA) were performed on a TGA 2950 TA Instruments (New Castle, Delaware, USA) under argon atmosphere (100 mL min⁻¹ flow rate). Samples were heated from 25°C to 700°C at a heating rate of 10°C min⁻¹.

Differential scanning calorimetry (DSC) measurements were performed on a DSC 2910 TA Instruments (New Castle, Delaware, USA), at heating and cooling rates of 20°C min⁻¹ in the temperature range from -100 to 200°C under argon atmosphere. Approximately 7 mg of the samples were weighed and sealed in aluminum pans. The following program was adopted for analysis: (I) heating from room temperature to 200°C, (II) 5 min isotherm, (III) cooling to -100°C, (IV) 5 min isotherm and (V) heating to 200°C under argon flow at 40 mL min⁻¹. Thermograms were normalized with respect to the sample mass.

Dynamic-mechanical thermal analyses (DMTA) were carried out on a DMTA V Rheometric Scientific (New Jersey, USA), in a tensile mode, 5°C min⁻¹ heating rate, 1.0 Hz, and amplitude of 0.05%. The samples of 7.9 x 10.00 x 0.9 mm³ dimensions were cooled to -80°C and heated to 200°C.

Swelling tests were performed with polyurethane film discs (8 mm diameter and 0.3 mm width) previously dried under vacuum. Dry discs were submerged in distilled water and kept in a thermostatic water bath (Julabo F12) for 24 h at constant temperatures (25, 35, 45 and 55°C). The swelling coefficient (Q) was calculated using Equation 1, where m_s and m_d are the mass of the swollen PU and the mass of the dry PU, respectively.

$$Q = (m_s / m_d) \times 100\% \quad (1)$$

Rheological measurements were conducted on a DHR2 Rheometer, TA Instruments, with steel parallel-plate geometry of 25mm diameter. In order to validate the linear domain, analyses were performed in oscillatory amplitude mode at the temperatures of 40°C and 100°C, with the strain varying from 0.001% to 1.5%, and from 0.0125% to 2.0%, respectively, and an angular frequency of 10.0 rad/s. For temperature sweep analyses, samples were cooled from 100°C to 50°C at a temperature step of 5°C, an angular frequency of 10.0 rad/s, and a soak time of 5 min.

3D printing was performed using a 6-axis robotic arm BioassemblyBot® (Advanced Solutions Life Sciences, USA). The printing temperature was fixed at 110 ± 1°C. PU-50%-PEtOx was used as a printing material loaded into a 30 CC cartridge (Nordson EFD, USA). The cartridges were fitted with a 920 µm diameter conical metallic nozzle (FISNAR) and extruded using a pneumatic pressure (80 psi). 3D printing was controlled with TSIM software (Advanced Solutions Life Sciences, V1.1.142, USA) at a printing speed of 0.48 mm/s. The STL file was sliced with TSIM (Advanced Solutions Life Sciences, USA).

For cell toxicity testing, human dermal fibroblasts were used. Foreskin samples were obtained from healthy patients undergoing circumcision, according to French regulation including a declaration to the ministry (DC No. 2014- 2281), and procurement of written informed consent from the patient. Fibroblasts were isolated from a 2 year-old donor and cultivated in flasks at 37°C, 5% CO₂ in Dulbecco's modified Eagle medium (DMEM)/Glutamax TM-1 medium (Gibco Cell Culture, Invitrogen, France), supplemented with 10% calf bovine serum (HyCloneTM, GE Healthcare Life Sciences, France), 1% penicillin, streptomycin, and amphotericine B (Bio Industries-Cliniscience, France). The culture medium was changed every 2 days and the cells were routinely passaged in culture flasks until usage. Cells of passages between 7 and 9 were used. For

cell toxicity assay, cells were seeded at a concentration of 170 000 cell/cm² in a 12-well plate and cultured until confluency. Once the confluence was reached, pieces of 3D printed PU-50%-PEtOx were weighed, deposited in each well, and kept in contact with the adherent cells for 24h. After 24h, the 3D printed pieces were removed and a LIVE/DEAD™ (Invitrogen, France) labelling of the remaining adherent cell sheet performed. Visible and fluorescent images were acquired using an Olympus IX51 microscope (Olympus, France). Cell viability was calculated as the ratio of LIVE to DEAD labelled cell numbers.

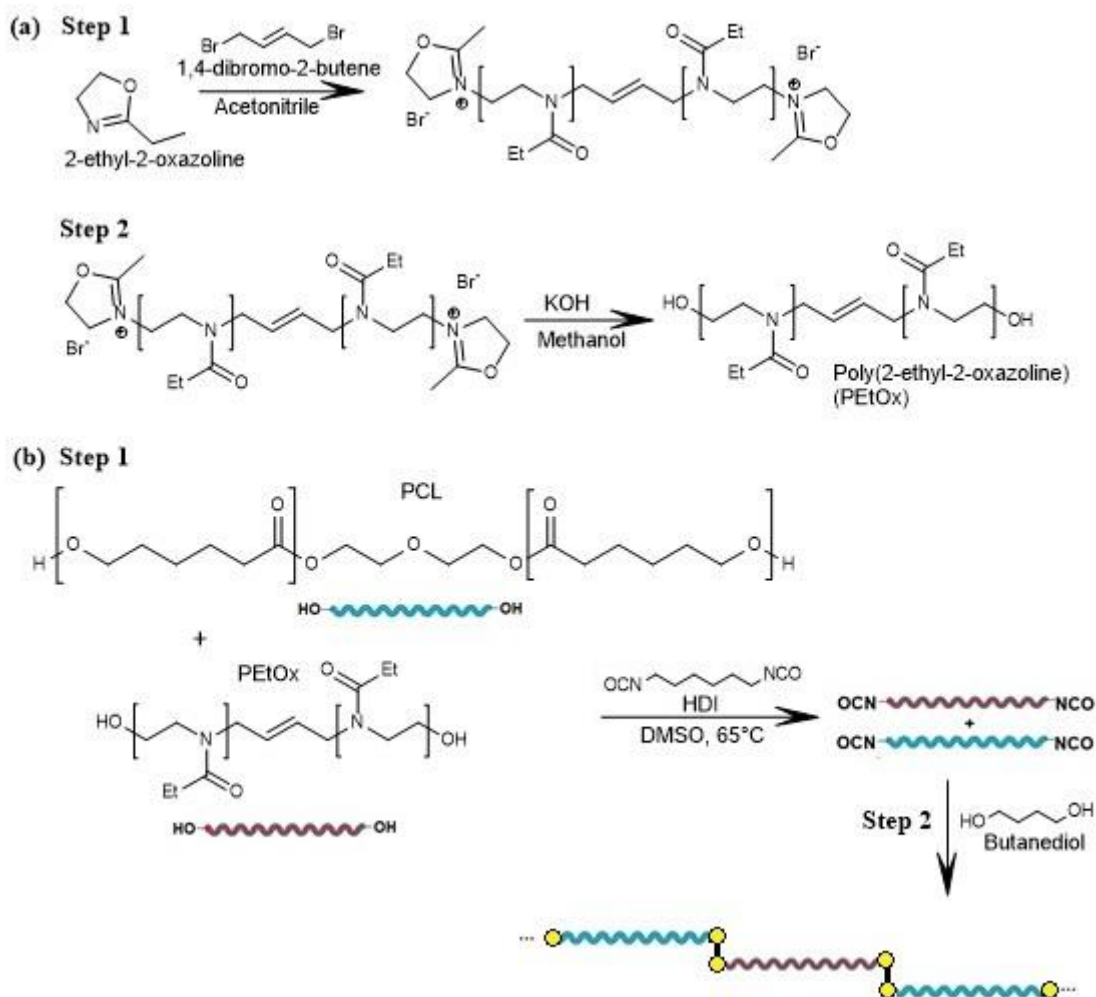
3. Results and Discussion

3.1. Synthesis

Dihydroxylated PEtOx was synthesized by cationic ring opening polymerization [38] using 1,4-dibromo-2-butene as a bifunctional and symmetric initiator (**Scheme 1a**). Polymerization resulted in PEtOx polyol with a narrow molar mass distribution ($\mathcal{D} = 1.4$) as determined by GPC, and with a yield of 90%. The PEtOx molar mass determined from ¹H NMR data was 4.0 kDa, equivalent to a degree of polymerization of 40. The signals in the ¹H NMR (**Figure S1**, Supporting Information) at 3.97 ppm, 2.83 ppm and 1.13 ppm were assigned to hydrogens H_a on the carbon of the initiator (-CH₂CH=), to H_b at the end group (HOCH₂-), and to H_c the pendent methyl groups of the mers (-CH₂CH₃), respectively. Polymer chain branching of PEtOx resulting from chain-transfer reactions has been reported in the literature. [39,62] Branching is undesirable for a polyol, because polyols with functionality higher than 2 lead to crosslinked polyurethanes. [8] However, the similarity of the integral values of the signals at 3.97 ppm and 2.83 ppm, and the narrow molar mass distribution of the PEtOx, indicates that the PEtOx polyol is linear.

Segmented polyurethanes were synthesized from commercial PCL-diol (2 kDa) and dehydroxylated PEtOx (**Scheme 1b**) at 60°C, to prevent by-products (e.g. allophanate and biuret, etc.), [63] under an argon atmosphere to guarantee the formation of linear polyurethanes. Segmented polyurethanes with different hydrophobic/hydrophilic balances were successfully prepared through different PCL/PEtOx mass ratios. The ¹H NMR spectrum of a PU prepared using a PCL/PEtOx mass ratio of 1:1 (PU-50%-PEtOx) and the assignment of the main signals, is shown in **Figure**

1. The signal at 4.07 ppm was assigned to H_a from the PCL segments, that at 3.47 ppm to the H_b from the PEtOx segments, and at 3.16 ppm, to the H_c from HDI fragments. ¹H NMR spectra of the other PUs can be found in **Figure S2 (Supporting Information)**. The composition of the PU, estimated from the relative areas of these signals (**Equations S1 and S2, Supporting Information**), is summarized in **Table 1**.



Scheme 1 – Synthesis of (a) of dihydroxylated PEtOx and (b) of segmented polyurethanes. The circles represent urethane linkages.

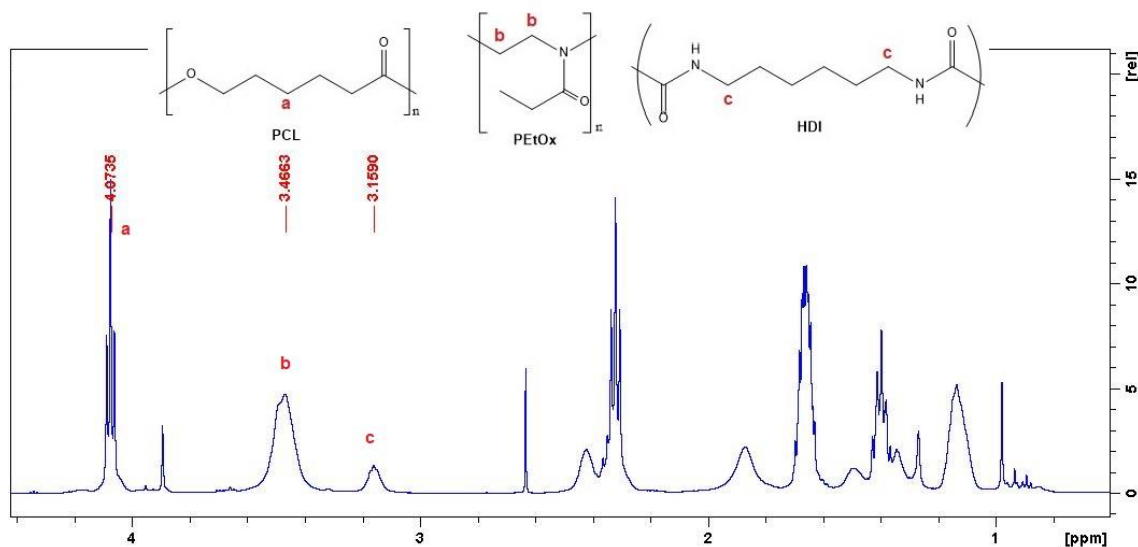


Figure 1 - ^1H NMR spectrum in CDCl_3 of PU-50%-PEtOx.

Table 1 – Nomenclature, PCL/PEtOx mass fraction in the reactional medium and in the PU, molar mass and dispersity, and thermal properties of the PU.

Nomenclature	PEtOx /PCL mass ratio (%)		Mn (kDa)	\bar{D}^{**}	T_g^1	T_g^2	T_m	T_c	T_{onset}
	Feed	PU*							
PCL	-	-	2.0* 4.0**	1.5	-56	-	40	18	240
PEtOx	-	-	4.0* 4.7**	1.4	-	55	-	-	270
PU-0%-PEtOx	0	0	39.6**	2.4	-49	-	40	-5	200
PU-25%-PEtOx	25.0	24.3	29.4**	2.5	-58	-	42	-	200
PU-50%-PEtOx	51.5	43.4	17.9**	2.6	-38	38	43	-	180
PU-75%-PEtOx	74.6	80.4	33.0**	4.0	-	29	-	-	220
PU-100%-PEtOx	100	100	12.9**	2.0	-	47	-	-	210

* Determined by ^1H NMR

** Determined by GPC in DMF

GPC chromatograms show a broad peak for PU-50%-PEtOx and a bimodal molar mass distribution for the other PU (Figure S3, Supporting Information). However, the molar mass dispersity \bar{D} of the PCL/PEtOx-based PUs varied in the range of 2.0 – 2.6, except for PU-75%-PEtOx, for which $\bar{D} = 4.0$ (Table 1), a characteristic behavior of

polyaddition. [4,63,64] The number average molar mass M_n varied in the range of 17.9 to 39.6 kDa, however no clear relation with the PU composition could be observed. ^1H NMR revealed that PEtOx contents in the PU were lower than in the feed ones. Both PCL and PEtOx present primary hydroxyls, therefore, the differences in the composition is not due to hydroxyl reactivity. However, PCL and PEtOx presented M_n values equal to 2 and 4 kDa, respectively, as determined by ^1H NMR. This difference possibly becomes more important as the polymerization proceeds and the viscosity of the reaction medium increases, affecting the polymerization kinetics due to diffusional control. [65] The higher molar mass of the PEtOx precursor imparts a higher viscosity, as predicted by the Mark-Houwink equation for diluted solutions. [66] This hypothesis of diffusional control on the PU composition is reinforced by comparing the M_n values of the PU from PCL and PEtOx, 36.9 kDa and 12.9 kDa for PU-0%-PEtOx and PU-100%-PEtOx, respectively; prepared under similar reaction conditions. Moreover, the molar mass dispersity presents an inverse behavior, and the lower dispersity for PU-100%-PEtOx is possibly due to a lower polymerization rate. [64,67]

3.2. Thermal and Mechanical Properties of the PCL/PEtOx-based PU

Segmented PU were thermally stable up to 200°C, being around 50 - 80°C less stable than PCL and PEtOx precursors, depending on the PU composition, as shown in **Figure S4 (Supporting Information)**. This is due to the introduction of carbamate linkages which degrade around 250°C for polyurethanes from HDI. [68] PU degraded in multi events at temperatures summarized in **Table S2 (Supporting Information)**. The onset temperature (T_{onset}) for the degradation of the PU is shown in **Table 1**.

DSC analyses were performed up to 200°C and the results are shown in **Figure 4**. While PEtOx is amorphous with a glass transition temperature (T_g) at 55°C, PCL is semicrystalline with T_g at -56°C and melting temperature (T_m) at 40°C. Segmented PUs are amorphous or semicrystalline, depending on the composition.

The first DSC heating scan for PU will be discussed together with the DMA data. The second heating scan for PU-100%-PEtOx (**Figure 2c**) showed only a glass transition close to the T_g of PEtOx, indicating the amorphous nature of this PU. PU-75%-PEtOx was also amorphous and the glass transition was shifted to lower temperatures compared with PU-100%-PEtOx, suggesting the miscibility of the PCL and PEtOx

segments in the PU. [69] However, the increase of PCL contents in the PU led to the formation of a PCL crystalline phase with T_m in the range of 40 – 43°C, close to the T_g for PU-0%-PEtOx and slightly lower than T_m of the PCL. A glass transition below -25°C can be observed in the DSC curves for PU containing PCL in the range of 50 – 100 wt.% and attributed to a PCL richer phase. The presence of such a phase with similar characteristics to the PLC precursor, suggests immiscibility and the existence of another phase. However, the glass transition of a second phase was probably overlapped by the melting of the PCL phase, as already described for PEtOx-*b*-PCL block copolymers. [70] The cooling curves (**Figure 2b**) evidenced a clear crystallization peak at -5°C for PU-0%-PEtOx.

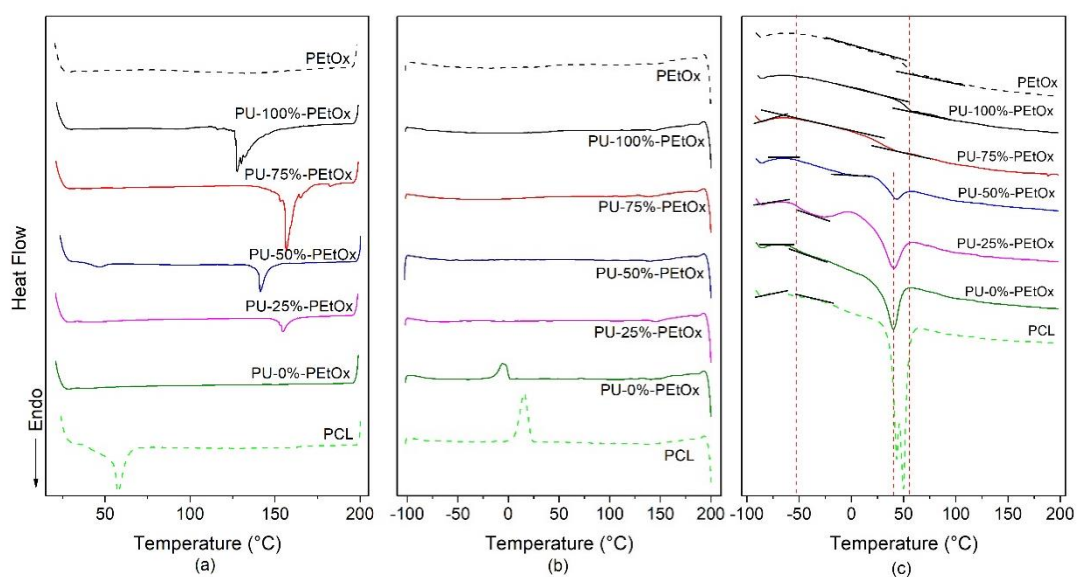


Figure 2 – DSC curves of the polyurethanes and macrodiol precursors. (a) First heat, (b) cooling and (c) second heat DSC curves.

Dynamical mechanical properties of segmented polyurethanes may be very complex due to the relaxations of the soft and hard segments, the presence of heterogeneities, and intermolecular interactions. [4,60,71] **Figure 3** shows storage (E') and loss (E'') moduli and loss factor ($\tan\delta$) of the segmented polyurethanes. For PU-0%-PEtOx, the storage modulus (**Figure 3a**) decreased continually from -70°C to 10°C, followed by a slight increase around 20°C, probably due to cold crystallization, and a second drop around 40°C due to the melting of PCL segments. Loss modulus curves (**Figure 3b**) presented a broad peak with a maximum at -53°C, attributed to the glass transition, and a second peak around 20°C followed by a drop at 27°C due to cold crystallization and melting, respectively. The cold crystallization was not observed in the

DSC first heating (**Figure 2a**) probably because the starting temperature of the first heating scan (room temperature) was close to the temperature range of the cold crystallization. The broadness of the glass transition of the PU-0%-PEtOx is highlighted in the loss factor curves, indicating a broad relaxation spectrum and suggesting the presence of different microenvironments. For PU-25%-PEtOx, the storage modulus also decreased continuously in the same temperature range, however cold crystallization was not present. The loss modulus curve showed an even broader peak, which possibly resulted from the overlap of peaks centred at -53°C and -20°C , indicated by arrows in **Figure 3b**. This hypothesis is reinforced by the tan delta curve which presented a peak at 0°C and shoulders at -50 and -40°C , attributed to the glass transitions of PEtOx and PCL richer phases. The storage modulus for the PU-50%- and -75%-PEtOx (**Figure 3b**) presented two drops starting around -40°C and 30°C , due to the glass transitions of PCL and PEtOx richer phases. On the other hand, the loss modulus showed a well-defined peak centered at 30°C and another less intense peak at around -40°C . From DSC and DMTA data, it is possible to conclude that segmented PU based on PCL and PEtOx are partially miscible, presenting one or more phases whose glass transitions were shifted from the values for one component. [72] PU-100%-PEtOx could not be analysed due to the lack of dimensional stability.

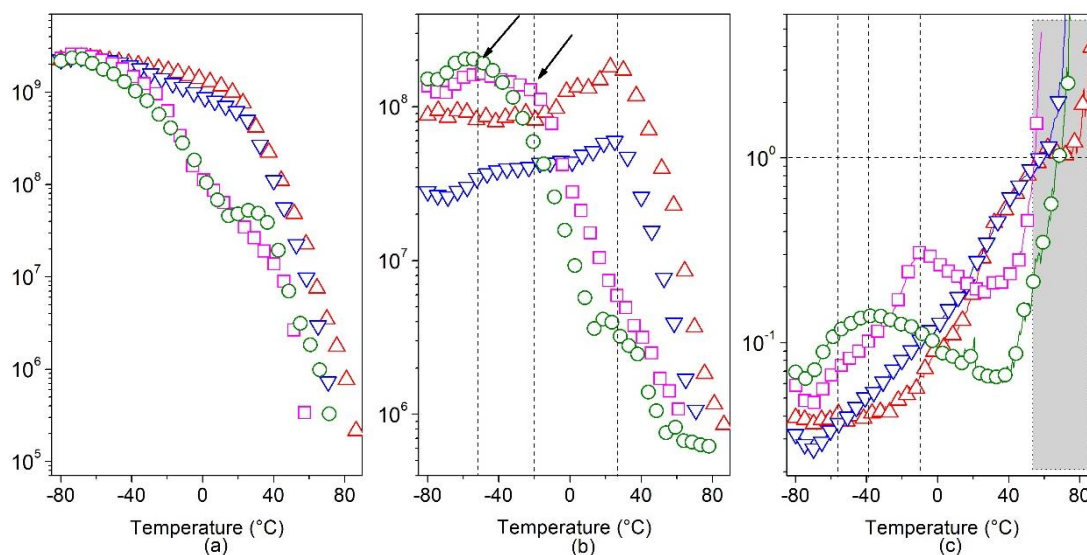


Figure 3 – (a) Storage and (b) loss moduli (Pa) and (c) loss factor ($\tan\delta$): Δ PU-75%-PEtOx, ∇ PU-50%-PEtOx, \square PU-25%-PEtOx, \circ PU-0%-PEtOx.

3.3. Swelling properties of the PCL/PETox-based PUs

PU synthesized with different PETox/PCL mass fractions are supposed to show particular characteristics, as already described for PETox-*b*-PCL amphiphilic block copolymers. These block copolymers are known to self-assemble in different morphologies depending on the mass fraction of the blocks. [42] Here, the combination of hydrophobic and hydrophilic polyols, PETox and PCL, respectively, resulted in amphiphilic and segmented polyurethanes, however with a random distribution of the segments or blocks. PU-based on PETox and PCL showed different water uptake capabilities, depending on the polyols mass fraction (**Figure 4**). The greater the mass fraction of the hydrophilic segment, the more water could be swollen. The swelling coefficient at 25°C varied in the range from 100 to 291% for PU-0%-PETox and PU-75%-PETox. PU-100%-PETox disintegrated during the swelling experiment due to the high sorption rate imparted by the high hydrophilicity, and the swelling coefficient could not be determined. Poly(oxazoline) presents a lower critical solution temperature (LCST) phase behavior in aqueous solution for a degree of polymerization higher than 100. [39,56,57] The degree of polymerization of the PETox precursor was 40, for which LCST behavior was not expected. However, the combination of PETox with hydrophobic PCL segments in a polyurethane chain resulted in a responsiveness of the segmented PU to temperature. This behavior has been reported for PETox-*b*-PCL block copolymers in which the increase of the mass fraction of PCL led to a lowering of the critical temperature of the aqueous solutions, and the formation of a gel. [73]

Figure 4 shows a decrease of the swelling coefficient from 291 to 246% with increasing temperature from 25°C to 55°C for PU-75%-PETox. For PU-50%-PETox, the swelling coefficient was practically constant, while PU-25%-PETox presented a slight decrease of Q with increasing temperature.

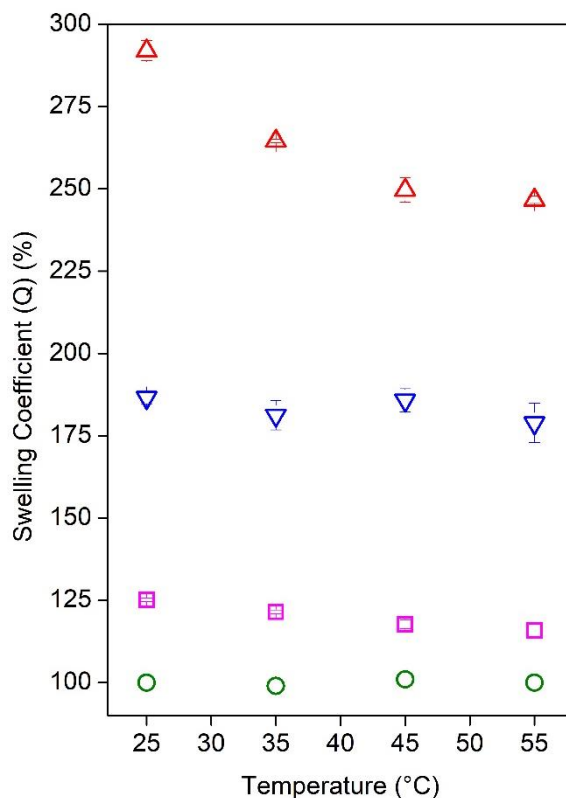


Figure 4 - Water swelling coefficient of the polyurethanes as a function of the temperature. \blacktriangle PU-75%-PEtOx, \blacktriangledown PU-50%-PEtOx, \blacksquare PU-25%-PEtOx, \circ PU-0%-PEtOx.

3.4. 3D Printing of the PCL/PEtOx-based PU:

Loss factor curves, determined by DMTA (**Figure 3c**), show that the segmented PU with different compositions presented a gel point, defined as the temperature in which $\tan(\delta) = 1$, in a narrow temperature range of 50 – 80°C (region highlighted by a gray rectangle). PU-50%-PEtOx was the PU of choice for 3D printing studies since it presents an intermediate composition and lower molar mass compared with the other PU (**Table 1**).

For FDM 3D printing, the temperature dependence of the rheological behaviour of a polymer is the key point for printability evaluation of any material. Rheological analysis was performed using the temperature sweep mode and a strain rate of 0.20%, which assures viscoelastic behavior for the temperature range studied, as determined by oscillatory amplitude assays (**Figure S5, Supporting Information**). The temperature range was chosen based on the DSC and DMTA data, in which 50°C is close to the glass transition of PU-50%-PEtOx, and above 60°C, this PU is supposedly molten.

So, decreasing the temperature from 100°C, both storage and loss moduli increase at different rates (**Figure 5**). The gelation temperature was more accurately determined from this experiment as 69°C. Below the gel temperature, molecular interactions between the chains retain the three-dimension structure and dimensional stability, while at higher temperatures, the density of these interactions is strongly reduced, allowing the melted polymer to flow. [74] In other words, 69°C is the minimum temperature to print PU-50%-PEtOx.

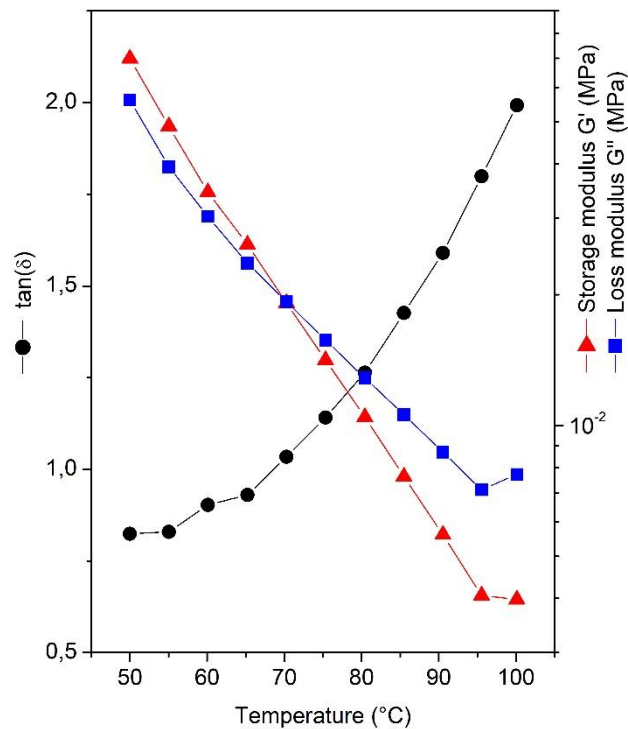


Figure 5 – Rheology: Temperature Sweep for PU-50%-PEtOx from 100°C to 50°C.

For the printing, simple computational designs (STL file) were used to optimize the printer parameters, such as temperature, pneumatic pressure, and the velocity of the printer. The main challenge was the high temperature required to melt the polymer and decrease the viscosity (complex viscosity of 2.8 kPa.s at 69°C). The printing was performed at 110°C to ensure the melting of the PU. The obtained viscosity at this temperature was around 0.9 Pa.s. Nevertheless, temperature loss from the nozzle tip toward the surrounding environment prevented the ideal flow, so forcing the use of a larger aperture nozzle (920 μm), leading to resolution loss. Besides, high elasticity of the molten polymer leads to the stretching of the extruded filament and to deformation of the object during printing, hindering the achievement of the 3D shapes with fidelity

towards the computational design. **Figure 6** shows the printed samples obtained using different parameters. The effect of the velocity on the quality of the printed objects is noticeable. A lower velocity (sample C) resulted in a higher fidelity shape compared to the computational project (STL). This result opened a broad perspective for 3D printing of biocompatible PCL/PETox-based polyurethane and promising possible applications for biomedical devices.

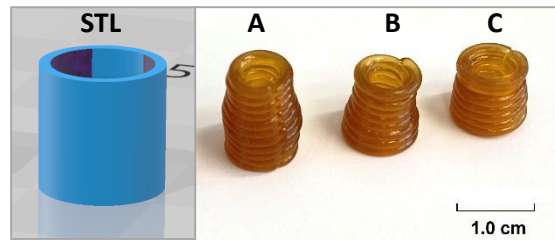


Figure 6 – STL: 1 cm diameter tube. Printed samples with different printing parameters: sample A: 84 psi and 0.60 mm/s; sample B: 80 psi and 0.55 mm/s; sample C: 80 psi and 0.48 mm/s.

3.5. Cell toxicology testing

The developed polyurethanes are composed of biocompatible polyols and aliphatic diisocyanate, which does not generate toxic metabolites in the body. [8,38,55] Nevertheless, cell viability in contact with the 3D printed filaments of PU-50%-PETox was evaluated and the results are presented in **Figure 7**. Cell viability loss was not detectable whatever the developed polyurethane quantities in contact with the cells for a period of 24 h. These results demonstrate the safety of the developed polyurethanes for biomedical applications.

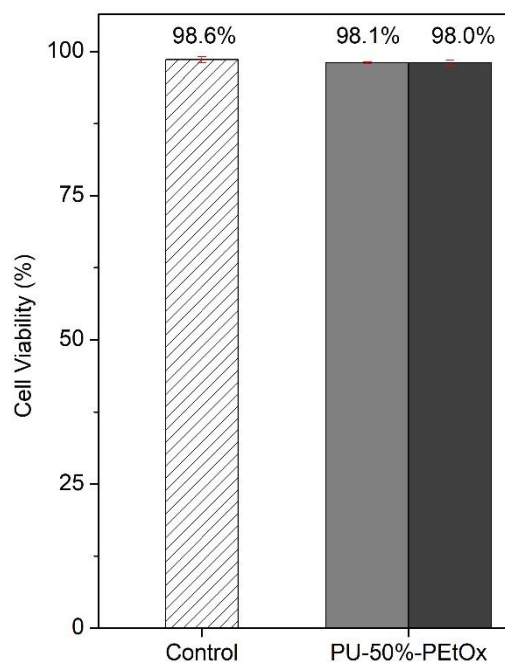


Figure 7 – Cell toxicology test of the PU-50%-PEtOx with different PU masses: ■ 62 mg, ■ 118mg. Control does not contain any polymer.

4. Conclusion

The synthesis of PCL/PEtOx based PU was successfully achieved, resulting in polymers with different polyols mass ratios, a number average molar mass in the range of 12.9 – 39.6 kDa, and a dispersity index between 2.0 and 4.0, values expected for a polyaddition. In general, the PCL mass fraction in the PU chains was higher than planned, suggesting that the PU composition was diffusion controlled because of the higher viscosity of the reaction medium, imparted by PEtOx rather than the PCL precursors. The segmented polyurethanes were heterogeneous, however, DSC and DMTA provided evidence of a partial miscibility. The combination of hydrophilic and hydrophobic segments into a PU chain imparted amphiphilicity and the capability of water uptake. Moreover, PU richer in PEtOx presented thermo-responsiveness. Cell viability testing showed that the PU are safe for biomedical applications. The 3D printing of PU-50%-PEtOx showed a promising application, even if the high viscoelasticity of the PU was found to be a real problem. The properties of these PUs, such as water swelling, mechanical properties, and biocompatibility, opens up a broad set of possible applications, from developing drug release systems, coating for medical devices, and furthermore, the 3D printing of medical devices themselves.

Acknowledgments:

The authors acknowledge the support from Fundação de Amparo à Pesquisa do Estado de São Paulo (FAPESP, Grant number 2015/25406-5; 2017/21231-1; 2017/03202-4; 2019/11372-2) and Dr. Emma Petiot for managing the cell toxicology tests at ICBMS – Université de Lyon.

5. References

- [1] Z.S. Petrovic, J. Ferguson, Polyurethanes elastomers, *Prog. Polym. Sci.* 16 (1991) 695–836. https://doi.org/10.1007/978-94-009-1531-2_60.
- [2] R.B. Seymour, G.B. Kauffman, Polyurethanes: A class of modern versatile materials, *J. Chem. Educ.* 69 (1992) 909–910. <https://doi.org/10.1021/ed069p909>.
- [3] D.K. Chattopadhyay, K.V.S.N. Raju, Structural engineering of polyurethane coatings for high performance applications, *Prog. Polym. Sci.* 32 (2007) 352–418. <https://doi.org/10.1016/j.progpolymsci.2006.05.003>.
- [4] R.B. Trinca, M.I. Felisberti, Segmented polyurethanes based on poly(L-lactide), poly(ethylene glycol) and poly(trimethylene carbonate): Physico-chemical properties and morphology, *Eur. Polym. J.* 62 (2015) 77–86. <https://doi.org/10.1016/j.eurpolymj.2014.11.008>.
- [5] L.P. Fonseca, R.B. Trinca, M.I. Felisberti, Amphiphilic polyurethane hydrogels as smart carriers for acidic hydrophobic drugs, *Int. J. Pharm.* 546 (2018) 106–114. <https://doi.org/10.1016/j.ijpharm.2018.05.034>.
- [6] C. Wang, Z. Yi, Y. Sheng, L. Tian, L. Qin, T. Ngai, W. Lin, Development of a novel biodegradable and anti-bacterial polyurethane coating for biomedical magnesium rods, *Mater. Sci. Eng. C* 99 (2019) 344–356. <https://doi.org/10.1016/j.msec.2019.01.119>.
- [7] J.O. Akindoyo, M.D.H. Beg, S. Ghazali, M.R. Islam, Polyurethane types, synthesis and applications – a review, *RSC Adv.* 6 (2016) 114453–114482. <https://doi.org/10.1039/c6ra14525f>.
- [8] L.P. Fonseca, R.B. Trinca, M.I. Felisberti, Thermo-responsive polyurethane hydrogels based on poly(ethylene glycol) and poly(caprolactone): Physico-chemical and mechanical properties, *J. Appl. Polym. Sci.* 133 (2016) 43573. <https://doi.org/10.1002/app.43573>.
- [9] M. Marzec, J. Kucińska-Lipka, I. Kalaszczyńska, H. Janik, Development of polyurethanes for bone repair, *Mater. Sci. Eng. C* 80 (2017) 736–747. <https://doi.org/10.1016/j.msec.2017.07.047>.
- [10] Y. Wen, N. Dai, S. Hsu, Biodegradable water-based polyurethane scaffolds with a sequential release function for cell-free cartilage tissue engineering, *Acta Biomater.* 88 (2019) 301–313. <https://doi.org/10.1016/j.actbio.2019.02.044>.
- [11] W. Jianhua, L. Shuen, W. Yanyan, T. Chunrong, Z. Xiuli, Mechanical and dynamic mechanical properties of degradable polyurethane foams with PEG/PCL mixed soft segments, *Adv. Mater. Res.* 183–185 (2011) 1611–1615. <https://doi.org/10.4028/www.scientific.net/AMR.183-185.1611>.

- [12] K. Kojio, S. Nozaki, A. Takahara, S. Yamasaki, Influence of chemical structure of hard segments on physical properties of polyurethane elastomers: a review, *J. Polym. Res.* 27 (2020) 64–67. <https://doi.org/10.1007/s10965-020-02090-9>.
- [13] M.M. Mirhosseini, V. Haddadi-asl, How the soft segment arrangement influences the microphase separation kinetics and mechanical properties of polyurethane block polymers, *Mater. Res. Express.* 6 (2019) 085311. <https://doi.org/https://doi.org/10.1088/2053-1591/ab1d73>.
- [14] I.S. Risti, I. Krakovský, D.T. Stojiljkovi, Crystallization and thermal properties in waterborne polyurethane elastomers : Influence of mixed soft segment block, *Mater. Chem. Phys.* 144 (2014) 31–40. <https://doi.org/10.1016/j.matchemphys.2013.12.008>.
- [15] R. Iyer, T. Nguyen, D. Padanilam, C. Xu, D. Saha, Glutathione-responsive biodegradable polyurethane nanoparticles for lung cancer treatment, *J. Control. Release.* 321 (2020) 363–371. <https://doi.org/10.1016/j.jconrel.2020.02.021>.
- [16] R.L.J. Cruz, M.T. Ross, S.K. Powell, M.A. Woodruff, Advancements in soft-tissue prosthetics part B : The chemistry of imitating life, *Front. Bioeng. Biotechnol.* 8 (2020) 1–23. <https://doi.org/10.3389/fbioe.2020.00147>.
- [17] S. Segan, M. Jakobi, P. Khokhani, S. Klimosch, F. Billing, M. Schneider, D. Martin, U. Metzger, A. Biesemeier, X. Xiong, A. Mukherjee, H. Steuer, B.M. Keller, T. Joos, M. Schmolz, U. Rothbauer, H. Hartmann, C. Burkhardt, G. Lorenz, N. Schneiderhan-Marra, C. Shipp, Systematic investigation of polyurethane biomaterial surface roughness on human immune responses in vitro, *Biomed Res. Int.* 2020 (2020) 1–15. <https://doi.org/10.1155/2020/3481549>.
- [18] D.S. Puperi, A. Kishan, Z.E. Punske, Y. Wu, E. Cosgriff-Hernandez, J.L. West, K.J. Grande-Allen, Electrospun polyurethane and hydrogel composite scaffolds as biomechanical mimics for aortic valve tissue engineering, *ACS Biomater. Sci. Eng.* 2 (2016) 1546–1558. <https://doi.org/10.1021/acsbiomaterials.6b00309>.
- [19] Y. Yao, D. Xu, C. Liu, Y. Guan, J. Zhang, Y. Su, L. Zhao, F. Meng, J. Luo, Biodegradable pH-sensitive polyurethane micelles with different polyethylene glycol (PEG) locations for anti-cancer drug carrier applications, *RSC Adv.* 6 (2016) 97684–97693. <https://doi.org/10.1039/c6ra20613a>.
- [20] X. He, M. Ding, J. Li, H. Tan, Q. Fu, L. Li, Biodegradable multiblock polyurethane micelles with tunable reduction-sensitivity for on-demand intracellular drug delivery, *RSC Adv.* 4 (2014) 24736–24746. <https://doi.org/10.1039/c4ra01478b>.
- [21] M. Sponchioni, U. Capasso Palmiero, D. Moscatelli, Thermo-responsive polymers: Applications of smart materials in drug delivery and tissue engineering, *Mater. Sci. Eng. C.* 102 (2019) 589–605. <https://doi.org/10.1016/j.msec.2019.04.069>.
- [22] T. Laube, J. Weisser, S. Berger, S. Börner, S. Bischoff, H. Schubert, M. Gajda, R. Bräuer, M. Schnabelrauch, In situ foamable, degradable polyurethane as biomaterial for soft tissue repair, *Mater. Sci. Eng. C.* 78 (2017) 163–174. <https://doi.org/10.1016/j.msec.2017.04.061>.
- [23] J. Herzberger, J.M. Serrine, C.B. Williams, T.E. Long, Polymer design for 3D printing elastomers: Recent advances in structure, properties, and printing, *Prog. Polym. Sci.* 97 (2019) 101144. <https://doi.org/10.1016/j.progpolymsci.2019.101144>.

- [24] S. Peng, Y. Li, L. Wu, J. Zhong, Z. Weng, L. Zheng, Z. Yang, J.T. Miao, 3D Printing mechanically robust and transparent polyurethane elastomers for stretchable electronic sensors, *ACS Appl. Mater. Interfaces*. 12 (2020) 6479–6488. <https://doi.org/10.1021/acsami.9b20631>.
- [25] W. Xu, X. Wang, Y. Yan, R. Zhang, Rapid prototyping of polyurethane for the creation of vascular systems, *J. Bioact. Compat. Polym.* 23 (2008) 103–114. <https://doi.org/10.1177/0883911507088271>.
- [26] H.A. Rather, R. Patel, U.C.S. Yadav, R. Vasita, Dual drug-delivering polycaprolactone-collagen scaffold to induce early osteogenic differentiation and coupled angiogenesis, *Biomed. Mater.* 15 (2020). <https://doi.org/10.1088/1748-605X/ab7978>.
- [27] R.S. Soufdoost, S.A. Mosaddad, Y. Salari, M. Yazdani, H. Tebyanian, E. Tahmasebi, A. Yazdani, A. Karami, A. Barkhordari, Surgical suture assembled with tadalafil/polycaprolactone drug-delivery for vascular stimulation around wound: Validated in a preclinical model, *Biointerface Res. Appl. Chem.* 10 (2020) 6317–6327. <https://doi.org/10.33263/BRIAC105.63176327>.
- [28] Y. Jin, P. Jong, H. Cha, S. Ik, B. So, Y. Kim, Clinical application of three-dimensionally printed biomaterial polycaprolactone (PCL) in augmentation rhinoplasty, *Aesthetic Plast. Surg.* 43 (2019) 437–446. <https://doi.org/10.1007/s00266-018-1280-1>.
- [29] K. Knop, R. Hoogenboom, D. Fischer, U.S. Schubert, Poly(ethylene glycol) in drug delivery: Pros and cons as well as potential alternatives, *Angew. Chemie - Int. Ed.* 49 (2010) 6288–6308. <https://doi.org/10.1002/anie.200902672>.
- [30] Q. Yang, S.K. Lai, Anti-PEG immunity: Emergence, characteristics, and unaddressed questions, *Wiley Interdiscip. Rev. Nanomedicine Nanobiotechnology*. 7 (2015) 655–677. <https://doi.org/10.1002/wnan.1339>.
- [31] M. Grube, M.N. Leiske, U.S. Schubert, I. Nischang, POx as an alternative to PEG? A hydrodynamic and light scattering study, *Macromolecules*. 51 (2018) 1905–1916. <https://doi.org/10.1021/acs.macromol.7b02665>.
- [32] O. Sedlacek, B.D. Monnery, S.K. Filippov, R. Hoogenboom, M. Hruby, Poly(2-oxazoline)s - Are they more advantageous for biomedical applications than other polymers?, *Macromol. Rapid Commun.* 33 (2012) 1648–1662. <https://doi.org/10.1002/marc.201200453>.
- [33] M. Barz, R. Luxenhofer, R. Zentel, M.J. Vicent, Overcoming the PEG-addiction: Well-defined alternatives to PEG, from structure-property relationships to better defined therapeutics, *Polym. Chem.* 2 (2011) 1900–1918. <https://doi.org/10.1039/c0py00406e>.
- [34] R. Hoogenboom, Poly(2-oxazoline)s: A polymer class with numerous potential applications, *Angew. Chemie - Int. Ed.* 48 (2009) 7978–7994. <https://doi.org/10.1002/anie.200901607>.
- [35] S. Huber, N. Hutter, R. Jordan, Effect of end group polarity upon the lower critical solution temperature of poly(2-isopropyl-2-oxazoline), *Colloid Polym. Sci.* 286 (2008) 1653–1661. <https://doi.org/10.1007/s00396-008-1942-7>.
- [36] T. Lorson, M.M. Lübtow, E. Wegener, M.S. Haider, S. Borova, D. Nahm, R. Jordan, M. Sokolski-Papkov, A. V. Kabanov, R. Luxenhofer, Poly(2-oxazoline)s based biomaterials: A comprehensive and critical update, *Biomaterials*. 178 (2018) 204–280.

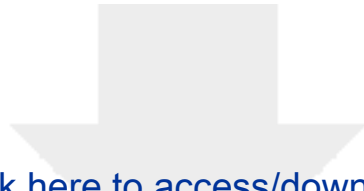
- <https://doi.org/10.1016/j.biomaterials.2018.05.022>.
- [37] M. Glassner, M. Vergaelen, R. Hoogenboom, Poly(2-oxazoline)s: A comprehensive overview of polymer structures and their physical properties, *Polym. Int.* 67 (2018) 32–45. <https://doi.org/10.1002/pi.5457>.
- [38] B. Verbraeken, B.D. Monnery, K. Lava, R. Hoogenboom, The chemistry of poly(2-oxazoline)s, *Eur. Polym. J.* 88 (2017) 451–469. <https://doi.org/10.1016/j.eurpolymj.2016.11.016>.
- [39] C. Gauche, M.I. Felisberti, Colloidal behavior of cellulose nanocrystals grafted with poly(2-alkyl-2-oxazoline)s, *ACS Omega.* 4 (2019) 11893–11905. <https://doi.org/10.1021/acsomega.9b01269>.
- [40] B. Guillerm, S. Monge, V. Lapinte, J.J. Robin, How to modulate the chemical structure of polyoxazolines by appropriate functionalization, *Macromol. Rapid Commun.* 33 (2012) 1600–1612. <https://doi.org/10.1002/marc.201200266>.
- [41] L. Bu, H. Zhang, K. Xu, B. Du, C. Zhu, Y. Li, pH and reduction dual-responsive micelles based on novel polyurethanes with detachable poly(2-ethyl-2-oxazoline) shell for controlled release of doxorubicin, *Drug Deliv.* 26 (2019) 300–308. <https://doi.org/10.1080/10717544.2019.1580323>.
- [42] U.U. Ozkose, S. Gulyuz, U.C. Oz, M.A. Tasdelen, O. Alpturk, A. Bozkir, O. Yilmaz, Development of Self-Assembled Poly(2-ethyl-2-oxazoline)-b-Poly(ϵ -caprolactone) (PEtOx-b-PCL) Copolymeric Nanostructures in Aqueous Solution and Evaluation of Their Morphological Transitions, *EXPRESS Polym. Lett.* 14 (2020) 1048–1062. <https://doi.org/https://doi.org/10.3144/expresspolymlett.2020.85>.
- [43] J. Yang, L. Li, C. Ma, X. Ye, Degradable polyurethane with poly(2-ethyl-2-oxazoline) brushes for protein resistance, *RSC Adv.* 6 (2016) 69930–69938. <https://doi.org/10.1039/c6ra13663j>.
- [44] M. Wu, Y. Zhang, H. Huang, J. Li, H. Liu, Z. Guo, L. Xue, S. Liu, Y. Lei, Assisted 3D printing of microneedle patches for minimally invasive glucose control in diabetes, *Mater. Sci. Eng. C.* 117 (2020) 111299. <https://doi.org/10.1016/j.msec.2020.111299>.
- [45] J. Yuan, P. Zhen, H. Zhao, K. Chen, X. Li, M. Gao, J. Zhou, X. Ma, The preliminary performance study of the 3D printing of a tricalcium phosphate scaffold for the loading of sustained release anti-tuberculosis drugs, *J. Mater. Sci.* 50 (2015) 2138–2147. <https://doi.org/10.1007/s10853-014-8776-0>.
- [46] N. Beheshtizadeh, N. Lotfibakhshaiesh, Z. Pazhouhnia, M. Hoseinpour, M. Nafari, A review of 3D bio-printing for bone and skin tissue engineering: a commercial approach, *J. Mater. Sci.* 55 (2020) 3729–3749. <https://doi.org/10.1007/s10853-019-04259-0>.
- [47] Y. Zhao, Y. Hou, Z. Li, Z. Wang, X. Yan, Powder-based 3D printed porous structure and its application as bone scaffold, *Front. Mater.* 7 (2020) 1–5. <https://doi.org/10.3389/fmats.2020.00150>.
- [48] P. Ramiah, L.C. du Toit, Y.E. Choonara, P.P.D. Kondiah, V. Pillay, Hydrogel-based bioinks for 3D bioprinting in tissue regeneration, *Front. Mater.* 7 (2020) 1–13. <https://doi.org/10.3389/fmats.2020.00076>.
- [49] Y.T. Wen, N.T. Dai, S. hui Hsu, Biodegradable water-based polyurethane scaffolds with a sequential release function for cell-free cartilage tissue engineering, *Acta Biomater.* 88 (2019) 301–313. <https://doi.org/10.1016/j.actbio.2019.02.044>.

- [50] C. Kaynak, S.D. Varsavas, Performance comparison of the 3D-printed and injection-molded PLA and its elastomer blend and fiber composites, *J. Thermoplast. Compos. Mater.* 32 (2018) 501–520. <https://doi.org/10.1177/0892705718772867>.
- [51] E.J. Courtial, C. Perrinet, A. Colly, D. Mariot, J.M. Frances, R. Fulchiron, C. Marquette, Silicone rheological behavior modification for 3D printing: Evaluation of yield stress impact on printed object properties, *Addit. Manuf.* 28 (2019) 50–57. <https://doi.org/10.1016/j.addma.2019.04.006>.
- [52] D.M. Senderoff, Biceps augmentation using solid silicone implants, *Aesthetic Surg. J.* 38 (2018) 401–408. <https://doi.org/10.1093/asj/sjx164>.
- [53] A. Gloria, B. Frydman, M.L. Lamas, A.C. Serra, M. Martorelli, J.F.J. Coelho, A.C. Fonseca, M. Domingos, The influence of poly(ester amide) on the structural and functional features of 3D additive manufactured poly(ϵ -caprolactone) scaffolds, *Mater. Sci. Eng. C.* 98 (2019) 994–1004. <https://doi.org/10.1016/j.msec.2019.01.063>.
- [54] J.Y. Cherng, T.Y. Hou, M.F. Shih, H. Talsma, W.E. Hennink, Polyurethane-based drug delivery systems, *Int. J. Pharm.* 450 (2013) 145–162. <https://doi.org/10.1016/j.ijpharm.2013.04.063>.
- [55] B.R. Barrioni, S.M. De Carvalho, R.L. Oréface, A.A.R. De Oliveira, M.D.M. Pereira, Synthesis and characterization of biodegradable polyurethane films based on HDI with hydrolyzable crosslinked bonds and a homogeneous structure for biomedical applications, *Mater. Sci. Eng. C.* 52 (2015) 22–30. <https://doi.org/10.1016/j.msec.2015.03.027>.
- [56] R. Hoogenboom, H.M.L. Thijs, M.J.H.C. Jochems, B.M. Van Lankvelt, M.W.M. Fijten, U.S. Schubert, Tuning the LCST of poly(2-oxazoline)s by varying composition and molecular weight: Alternatives to poly(N-isopropylacrylamide)?, *Chem. Commun.* (2008) 5758–5760. <https://doi.org/10.1039/b813140f>.
- [57] C. Weber, R. Hoogenboom, U.S. Schubert, Temperature responsive bio-compatible polymers based on poly(ethylene oxide) and poly(2-oxazoline)s, *Prog. Polym. Sci.* 37 (2012) 686–714. <https://doi.org/10.1016/j.progpolymsci.2011.10.002>.
- [58] R. Hoogenboom, Poly(2-oxazoline)s: Alive and kicking, *Macromol. Chem. Phys.* 208 (2007) 18–25. <https://doi.org/10.1002/macp.200600558>.
- [59] D. Christova, R. Velichkova, E.J. Goethals, F.E. Du Prez, Amphiphilic segmented polymer networks based on poly(2-alkyl-2-oxazoline) and poly(methyl methacrylate), *Polymer (Guildf)*. 43 (2002) 4585–4590. [https://doi.org/10.1016/S0032-3861\(02\)00313-0](https://doi.org/10.1016/S0032-3861(02)00313-0).
- [60] G.M.S. Paiva, L.G.T.A. Duarte, M.M. Faleiros, T.D.Z. Atvars, M.I. Felisberti, Z-E isomerization of azobenzene based amphiphilic poly(urethane-urea)s: Influence on the dynamic mechanical properties and the effect of the self-assembly in solution on the isomerization kinetics, *Eur. Polym. J.* 127 (2020) 109583. <https://doi.org/10.1016/j.eurpolymj.2020.109583>.
- [61] H. Kricheldorf, J. Meier-Haack, ABA triblock copolymers of L-lactide and poly(ethylene glycol), *Makromol. Chemie.* 194 (1993) 715–725. <https://doi.org/10.1002/macp.1993.021940229>.
- [62] J.M. Warakowski, B.P. Thill, Evidence for long chain branching in polyethyloxazoline, *J. Polym. Sci. Part A Polym. Chem.* 28 (1990) 3551–3563. <https://doi.org/10.1002/pola.1990.080281303>.
- [63] P. Król, Synthesis methods, chemical structures and phase structures of linear polyurethanes.

- Properties and applications of linear polyurethanes in polyurethane elastomers, copolymers and ionomers, *Prog. Mater. Sci.* 52 (2007) 915–1015. <https://doi.org/10.1016/j.pmatsci.2006.11.001>.
- [64] L. Polo Fonseca, M.I. Felisberti, Dynamic urea bond mediated polymerization as a synthetic route for telechelic low molar mass dispersity polyurethanes and its block copolymers, *Eur. Polym. J.* 118 (2019) 213–221. <https://doi.org/10.1016/j.eurpolymj.2019.05.052>.
- [65] H.U. Moritz, Increase in viscosity and its influence on polymerization processes, *Chem. Eng. Technol.* 12 (1989) 71–87. <https://doi.org/10.1002/ceat.270120112>.
- [66] J. Tóthová, K. Paulovičová, V. Lisý, Viscosity measurements of dilute poly(2-ethyl-2-oxazoline) aqueous solutions near theta temperature analyzed within the joint Rouse-Zimm model, *Int. J. Polym. Sci.* 2015 (2015). <https://doi.org/10.1155/2015/690136>.
- [67] L.P. Fonseca, D.D.M. Zanata, C. Gauche, M.I. Felisberti, A one-pot, solvent-free, and controlled synthetic route for thermoresponsive hyperbranched polyurethanes, *Polym. Chem.* 11 (2020) 6295–6307. <https://doi.org/10.1039/d0py01026j>.
- [68] D.K. Chattopadhyay, D.C. Webster, Thermal stability and flame retardancy of polyurethanes, *Prog. Polym. Sci.* 34 (2009) 1068–1133. <https://doi.org/10.1016/j.progpolymsci.2009.06.002>.
- [69] A.C. Quental, F.P. De Carvalho, E. Dos Santos Tada, M.I. Felisberti, Blends of PHB and its copolymers: miscibility and compability, *Quim. Nova.* 33 (2010) 438–446. <https://doi.org/10.1590/S0100-40422010000200035>.
- [70] S. Gulyuz, U.U. Ozkose, P. Kocak, D. Telci, O. Yilmaz, M.A. Tasdelen, In-vitro cytotoxic activities of poly(2-ethyl-2-oxazoline)-based amphiphilic block copolymers prepared by CuAAC click chemistry, *EXPRESS Polym. Lett.* 12 (2018) 146–158. <https://doi.org/10.3144/expresspolymlett.2018.13>.
- [71] R.B. Trinca, M.I. Felisberti, Effect of diisocyanates and chain extenders on the physicochemical properties and morphology of multicomponent segmented polyurethanes based on poly(l-lactide), poly(ethylene glycol) and poly(trimethylene carbonate), *Polym. Int.* 64 (2015) 1326–1335. <https://doi.org/10.1002/pi.4920>.
- [72] S.C. Cassu, M.I. Felisberti, Dynamic mechanical behavior and relaxations in polymers and polymeric blends, *Quim. Nova.* 28 (2005) 255–263. <https://doi.org/http://dx.doi.org/10.1590/S0100-40422005000200017>.
- [73] C. Kim, S.C. Lee, S.U.K.W.O.N. Kang, I.C.K.C. Kwon, S.E.O.Y. Jeong, Phase-transition characteristics of amphiphilic poly (2- ethyl-2-oxazoline)/ poly (ε-caprolactone) block copolymers, *J. Polym. Sci. Part B.* 38 (2000) 2400–2408. [https://doi.org/10.1002/1099-0488\(20000915\)38:18<2400::AID-POLB70>3.0.CO;2-7](https://doi.org/10.1002/1099-0488(20000915)38:18<2400::AID-POLB70>3.0.CO;2-7).
- [74] K. Nishinari, Rheological and DSC study of sol-gel transition in aqueous dispersions of industrially important polymers and colloids, *Colloid Polym. Sci.* 275 (1997) 1093–1107. <https://doi.org/10.1007/s003960050189>.

Declaration of Competing Interest

The authors declare that they have no known competing financial interests or personal relationships that could have appeared to influence the work reported in this paper



[Click here to access/download](#)

Supplementary Material

[Supporting Information_22_11_2020.docx](#)

